mvt@lisbon - 18 October 2011

Bio-optical Algorithms for European Seas: Performance and Applicability of Neural-Net Inversion Schemes

Davide D'Alimonte and Tamito Kajiyama

with the collaboration of

Giuseppe Zibordi, Jean-François Berthon, Frédéric Mélin and Elisabetta Canuti

Outline

- This study uses bio-optical algorithms (MLPs) to assess MERIS ocean color products in the Northern Adriatic Sea, the Baltic Sea and the Western Black Sea
- Research objectives included:
  - Dataset selection and quality assurance
  - Assessment of the MLP performance and applicability
  - Comparisons with MERIS products

Dataset selection

- Reference field measurements are the BiOMaP and CoASTS data, produced by the JRC and accessible within the framework of specific collaborations between JRC and FCT/UNL for MERIS products validation
- Complementary benchmark analyses were also undertaken on the basis of the NASA Bio-Optical Marine Data Set (NOMAD)

Dataset selection (cont.)

- The selection of BiOMaP and CoASTS data was supported by:
  - Novel methods for the quality assurance of in-situ measurements of absorption, attenuation and back-scattering
  - MC simulations of the radiative transfer process in the water medium to investigate uncertainties induced by sea-surface wave focusing on radiometric data products derived from free-fall optical systems
  - Use of AERONET-OC measurements to assess the quality of MERIS radiometric products

MLP bio-optical algorithms

- Operational MLPs were implemented to derive Chl-a, $a_{ys}(412)$ and TSM from L_{WN} on the basis of BiOMaP and CoASTS data
- MLP performance was assessed through:

$$\varepsilon = 100 \frac{1}{N} \sum_{i=1}^{N} \frac{\left| \hat{t}_i - t_i \right|}{t_i} \qquad \delta = 100 \frac{1}{N} \sum_{i=1}^{N} \frac{\hat{t}_i - t_i}{t_i}$$

- MLP parameter tables have been produced to permit user implementations of the bio-algorithms, and their application to MERIS images

MLP parameter tables

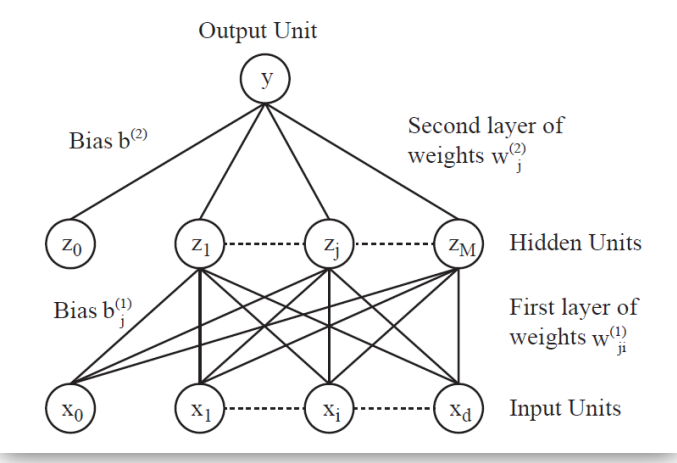


```
% Pre-processing
l = log10(RRS);
ndata = size(l, 1);
tmp = l-repmat(mu_l, ndata, 1);
x = tmp ./ repmat(s_l, ndata, 1);

% MLP mapping
z = tanh(x*net.w1 + ones(ndata, 1)*net.b1);
y = z*net.w2 + ones(ndata, 1)*net.b2;

% Post-processing
tmp = y.*repmat(s_c, ndata, 1);
c = 10^(tmp+repmat(mu_c, ndata, 1));
```

$$\mu_l = [\ -2.4140 \quad -2.3562 \quad -2.2420 \quad -2.2459 \quad -2.3001 \quad -3.1077\ ]$$

$$\sigma_l = [\ 0.1266 \quad 0.1376 \quad 0.1410 \quad 0.1531 \quad 0.1913 \quad 0.2898\ ]$$

$$w^{(1)} = \begin{bmatrix} 0.8171 & 0.1020 & 0.0055 & -0.7657 & 1.3000 & 0.9552 & -0.0389 & 0.2977 & -0.3111 & -1.3794 \\ 0.7788 & -0.8233 & -0.1462 & 1.0440 & -0.0541 & 0.5041 & 0.2709 & -0.2039 & -0.9394 & 0.2407 \\ -0.5943 & 0.2567 & 0.1180 & -0.0121 & -0.5634 & 0.0795 & 0.3766 & -0.0012 & -0.2342 & 0.5870 \\ 0.9183 & -0.2228 & -0.2723 & -0.3433 & 0.7181 & -0.3145 & -0.2038 & -0.8187 & -0.7295 & 0.2357 \\ 1.1696 & 0.0653 & -0.0641 & -0.4761 & 0.2034 & -0.4225 & 0.5823 & 0.5535 & -0.9467 & -1.6642 \\ -0.0250 & 0.4470 & 0.6222 & 0.3024 & -0.2759 & -0.4216 & 0.7834 & 0.2380 & -0.3021 & -0.2630 \end{bmatrix}$$

$$b^{(1)} = [\ 0.6897 \quad 0.4251 \quad -0.1718 \quad -0.5192 \quad 0.0070 \quad -0.0633 \quad -0.0405 \quad -0.7154 \quad -0.0193 \quad 0.0832\ ]$$

$$(w^{(2)})^T = [\ -0.5005 \quad 1.0459 \quad 1.1365 \quad -1.5768 \quad -0.0562 \quad 0.5799 \quad 0.7121 \quad 1.1483 \quad -0.9814 \quad 1.2666\ ] \text{ and } b^{(2)} = -0.0907$$

$$\mu_c = -0.0185 \text{ and } \sigma_c = 0.3270$$

http://www1.aston.ac.uk/eas/reSearch/groups/ncrg/resources/netlab

http://publications.jrc.ec.europa.eu/repository/handle/111111111/22406

Northern Adriatic Sea

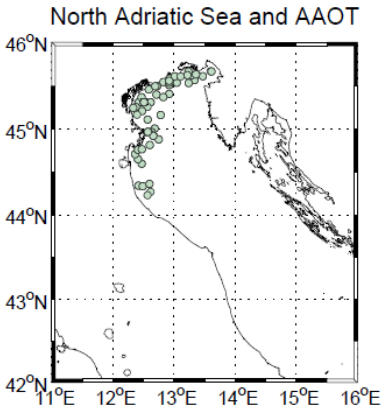

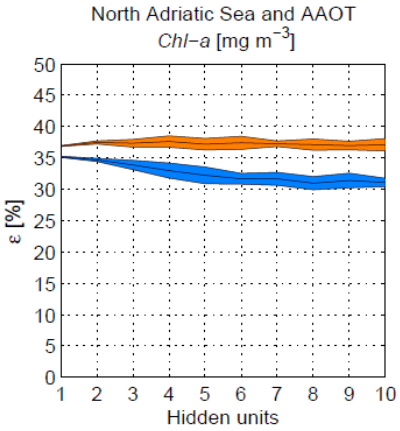

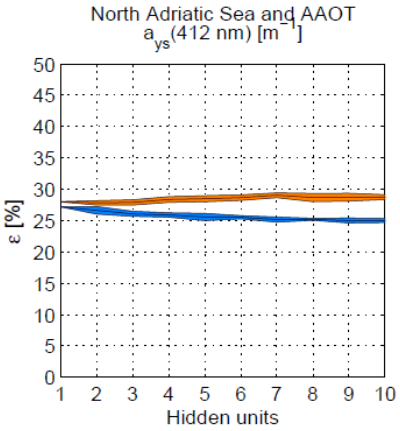

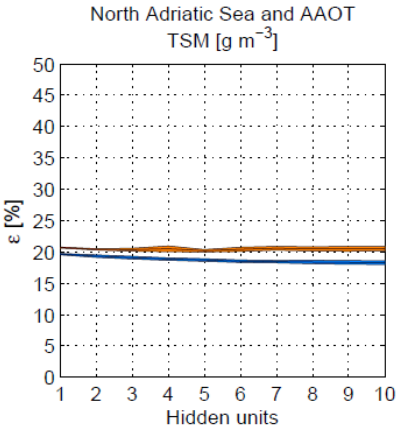

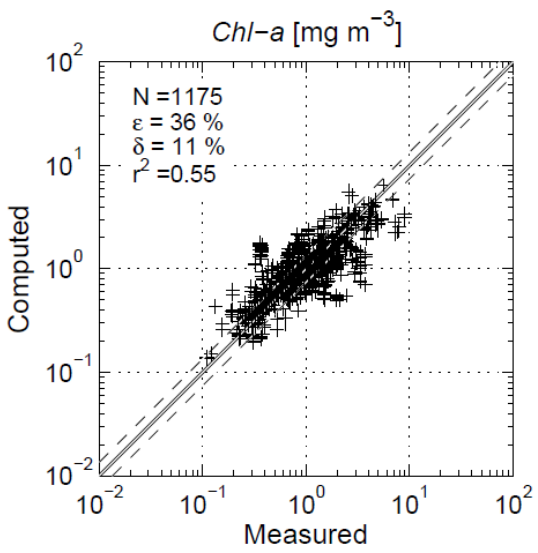

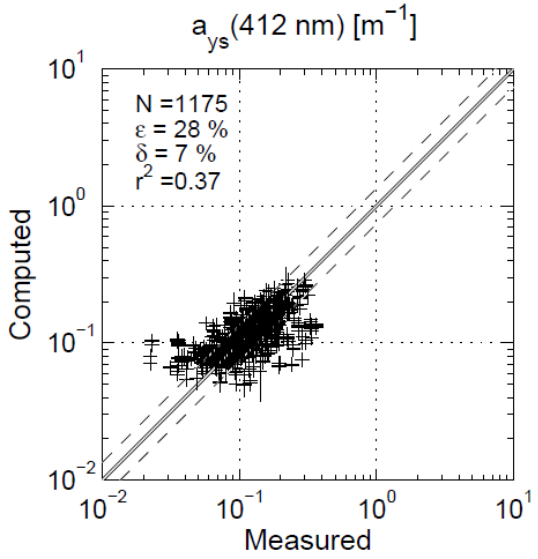

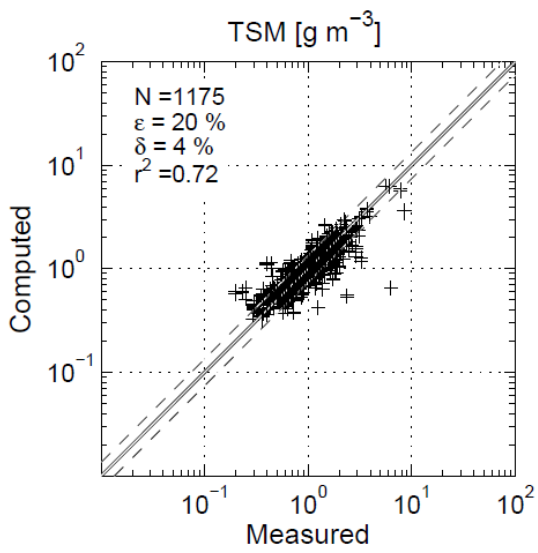

Eastern Mediterranean Sea

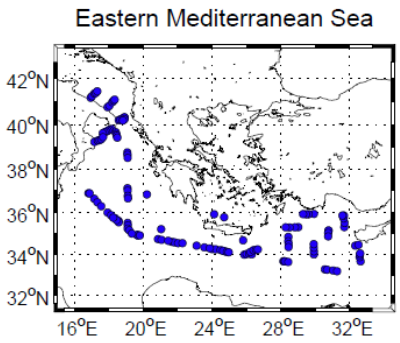

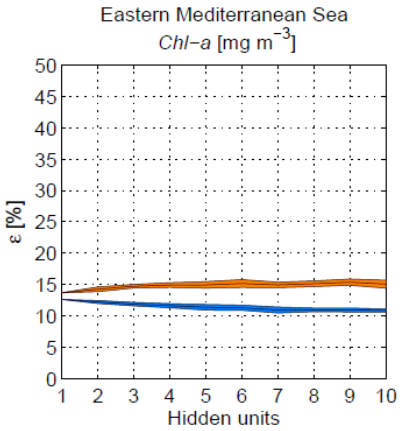

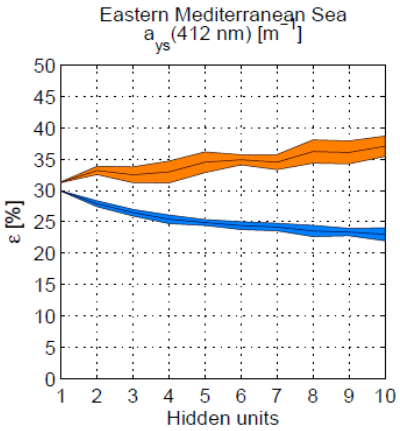

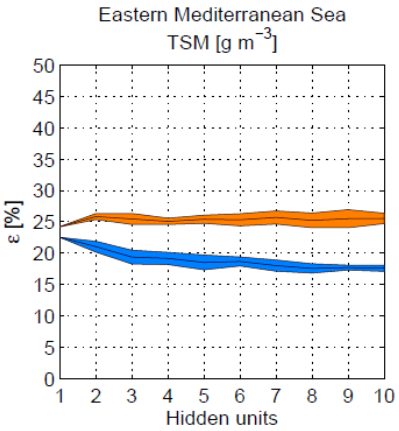

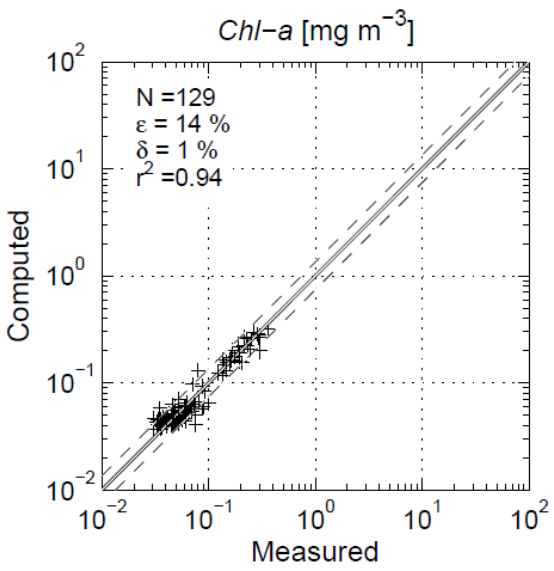

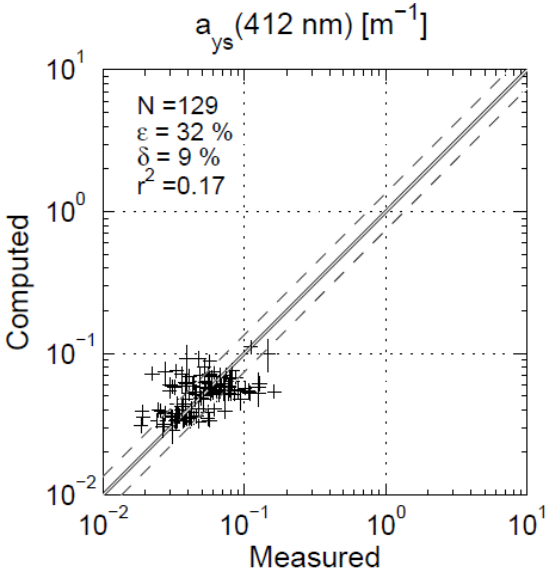

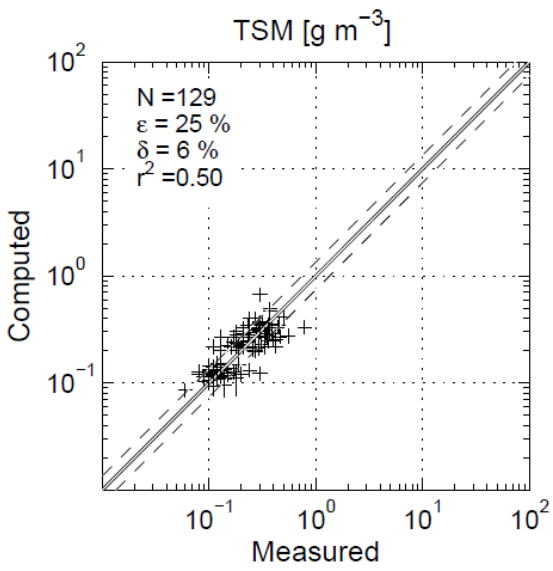

Western Black Sea

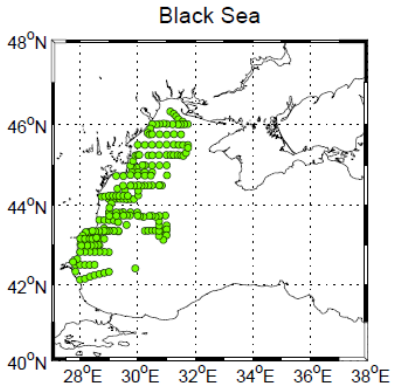

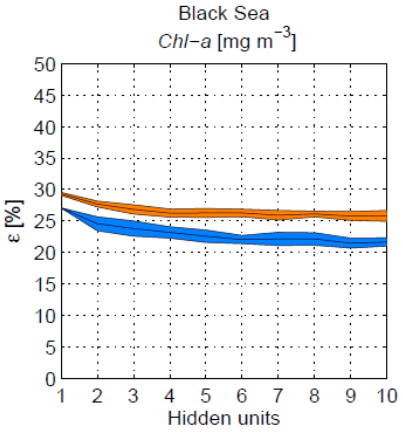

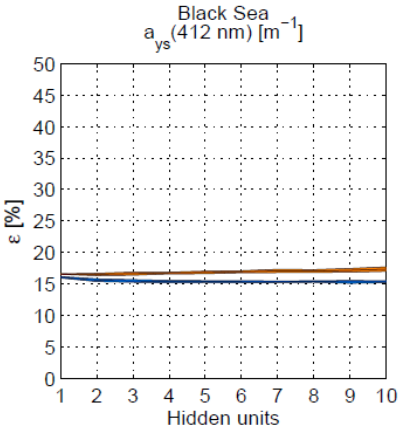

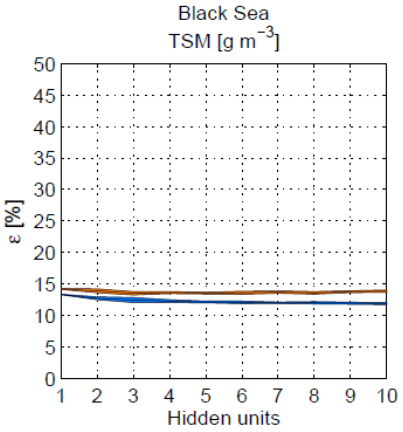

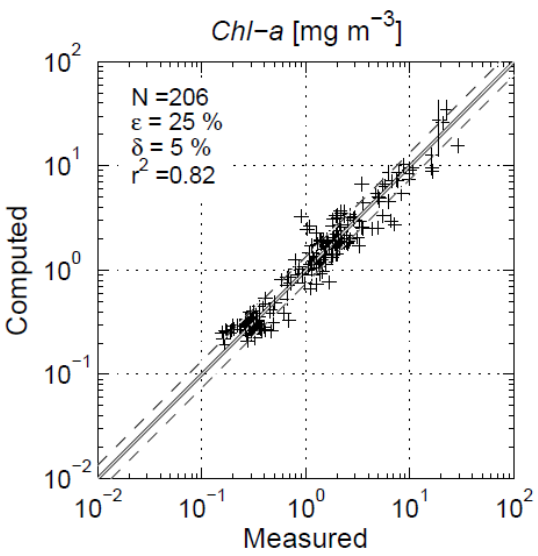

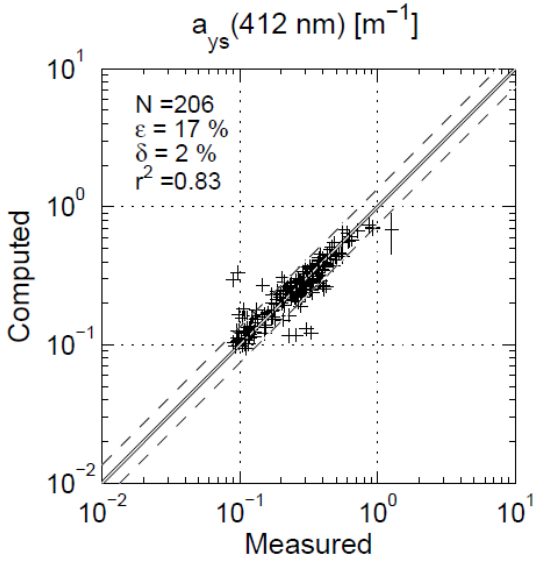

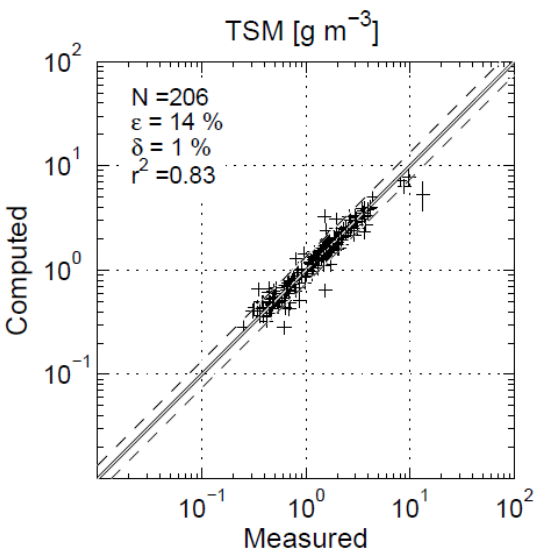

Baltic Sea

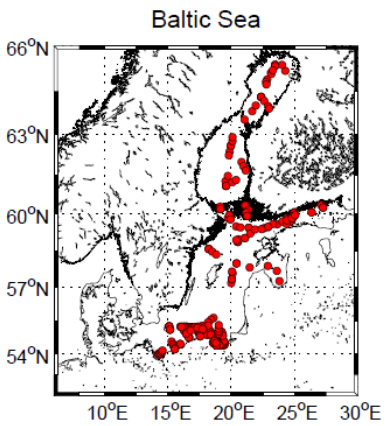
Baltic Sea
66°N
63°N
60°N
57°N
54°N
10°E
15°E
20°E
25°E
30°E

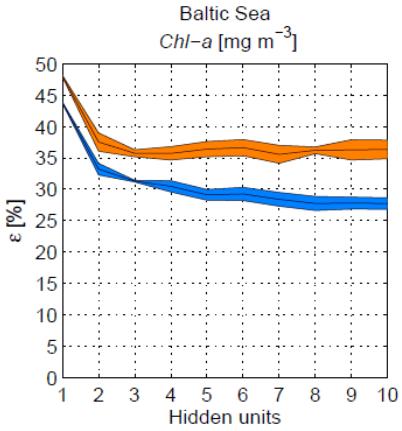
Baltic Sea
Chl−a [mg m−3]
ε [%]
Hidden units

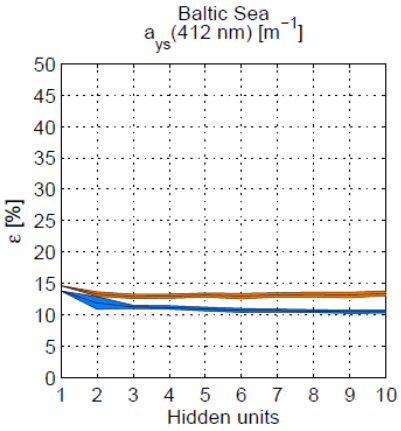
Baltic Sea
a ys(412 nm) [m−1]
ε [%]
Hidden units

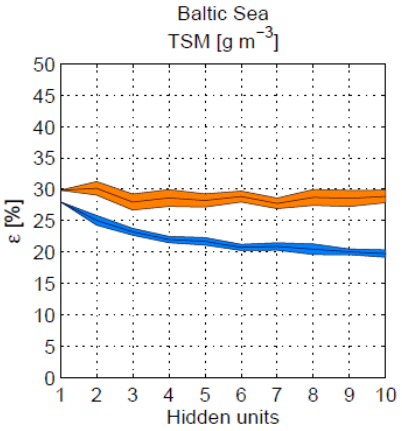
Baltic Sea
TSM [g m−3]
ε [%]
Hidden units

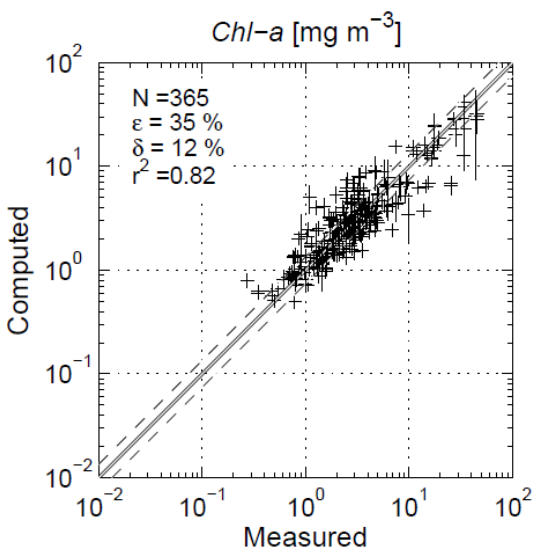
Chl−a [mg m−3]
N =365
ε = 35 %
δ = 12 %
r2 =0.82
Computed
Measured

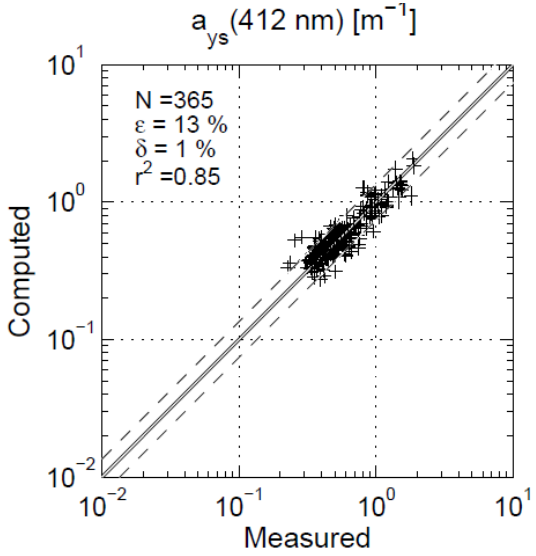
a ys(412 nm) [m−1]
N =365
ε = 13 %
δ = 1 %
r2 =0.85
Computed
Measured

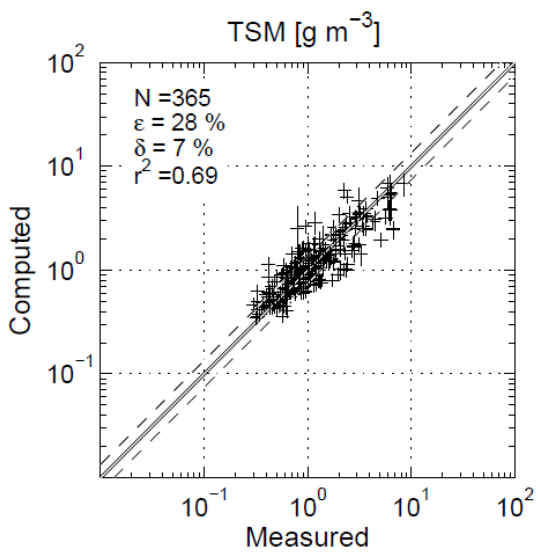
TSM [g m−3]
N =365
ε = 28 %
δ = 7 %
r2 =0.69
Computed
Measured

Performance analysis

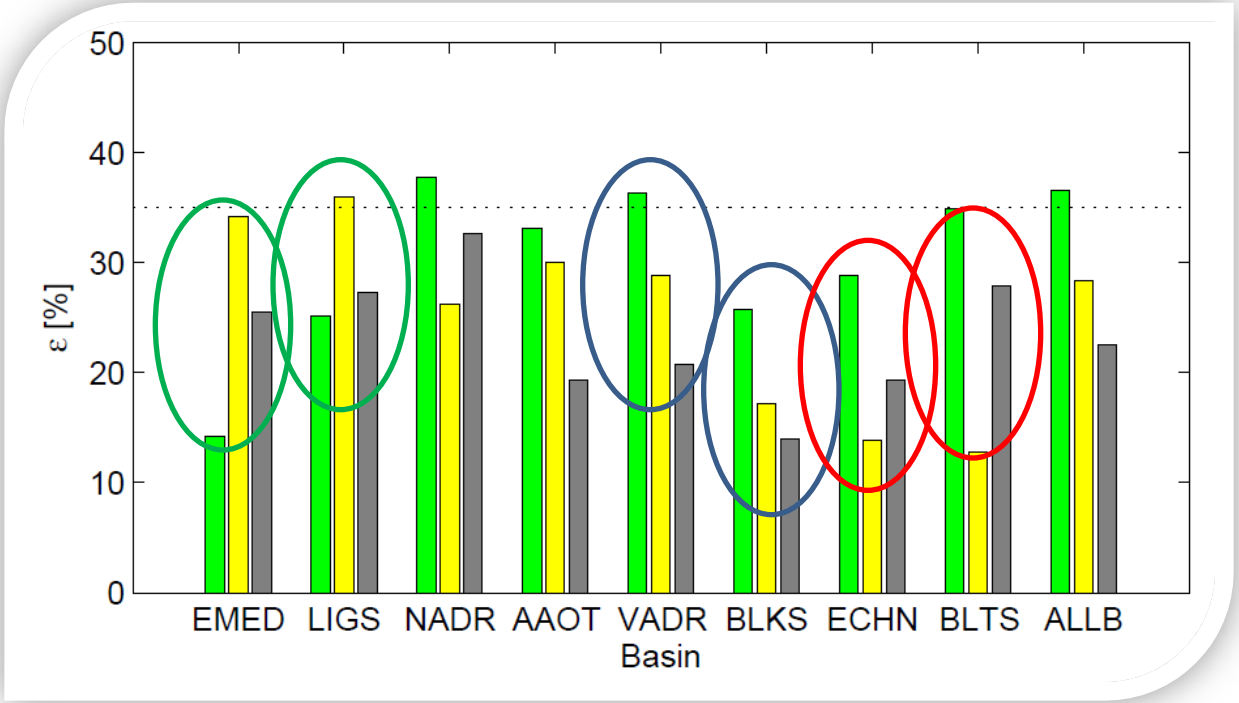

- Cross-validation results at individual basins and for the BiOMaP data ensemble
- Results for Chl-a, $a_{ys}(412)$ and TSM are in green, yellow and gray, respectively

Cross-basin applicability analysis

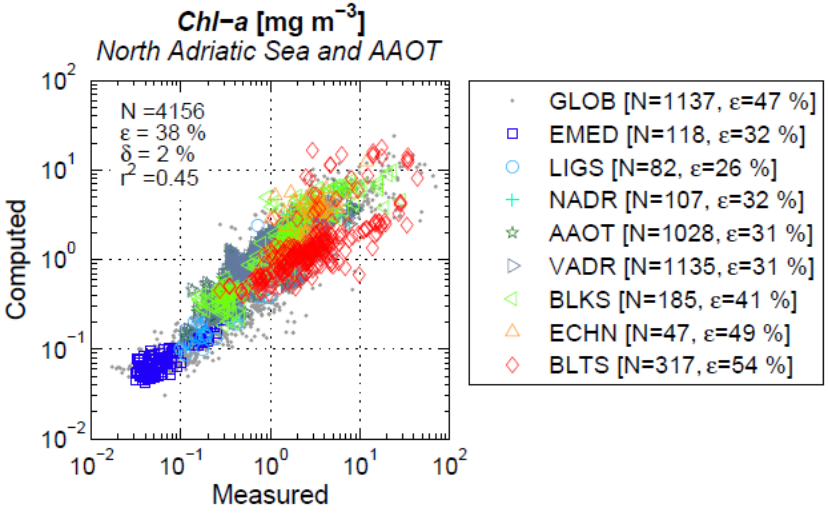

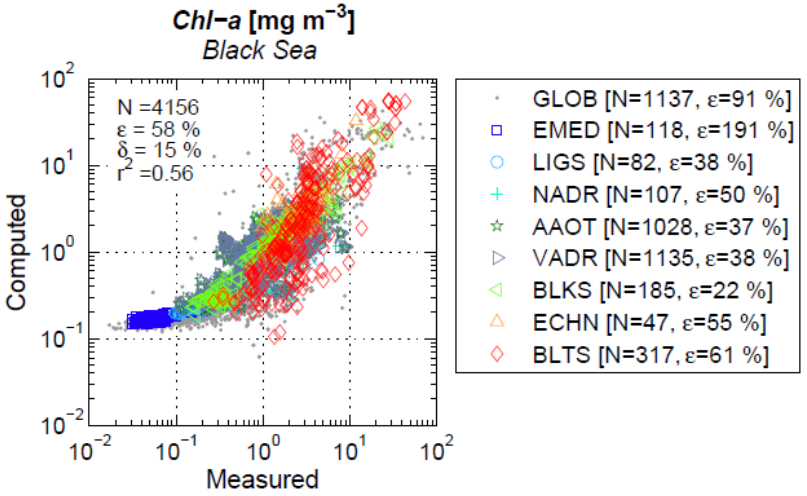

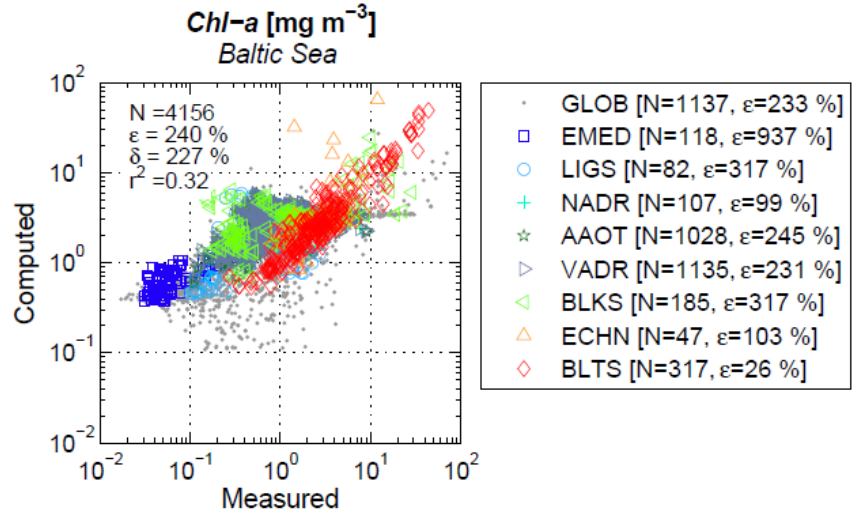

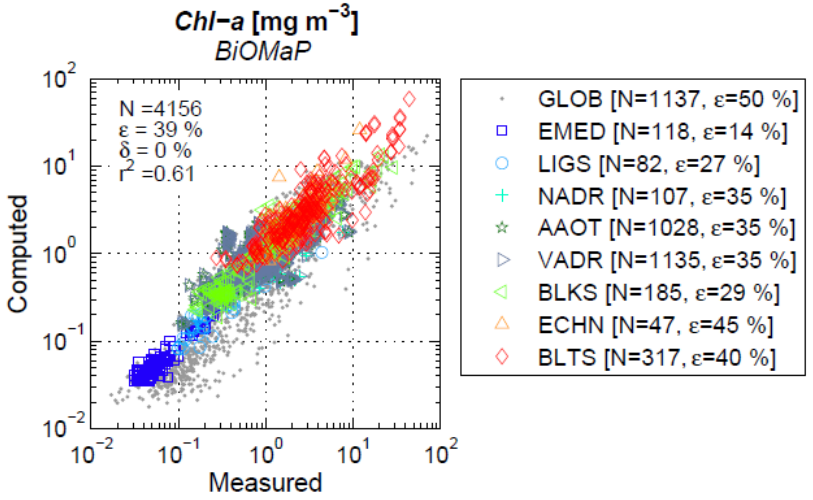

Cross-basin applicability analysis (cont.)

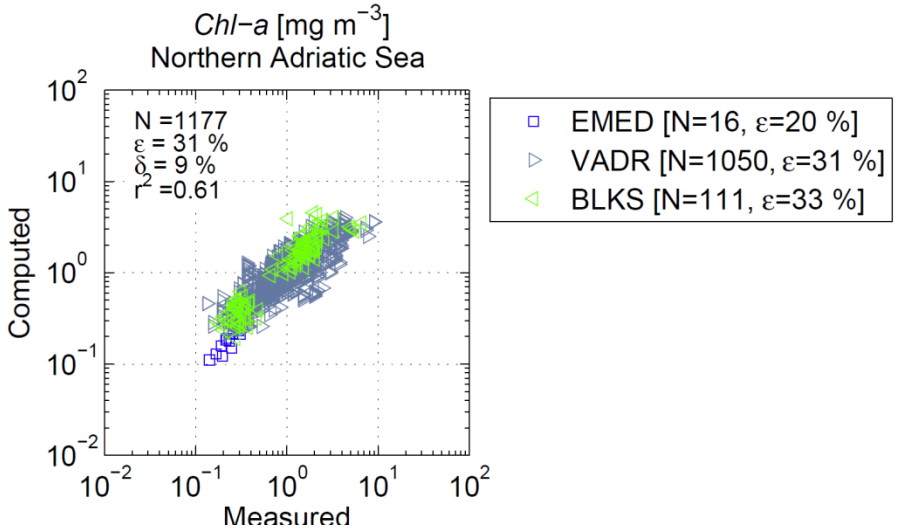

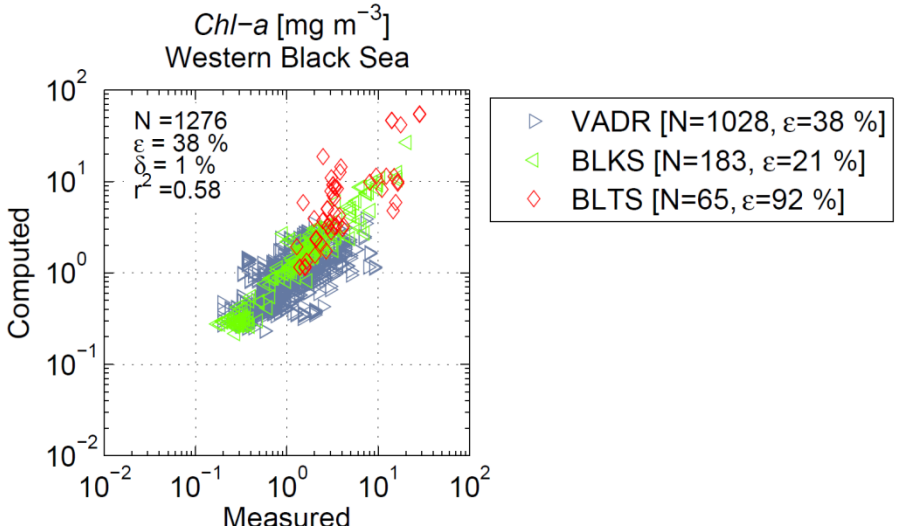

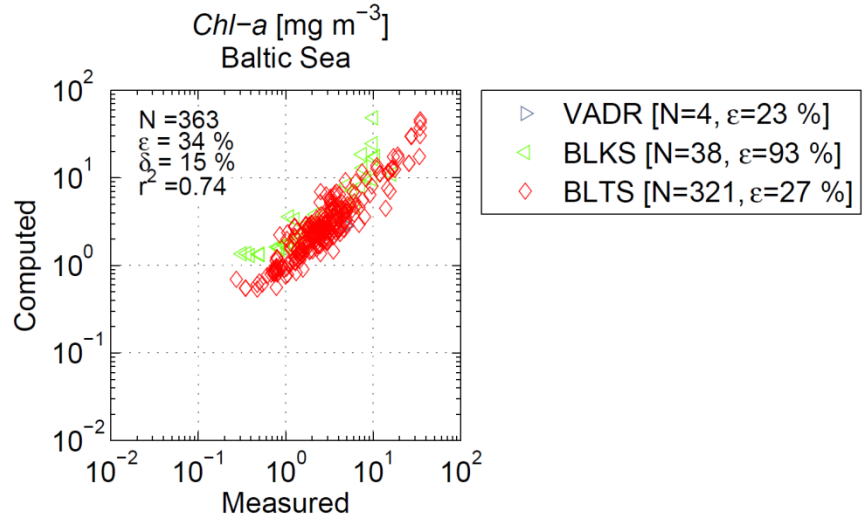

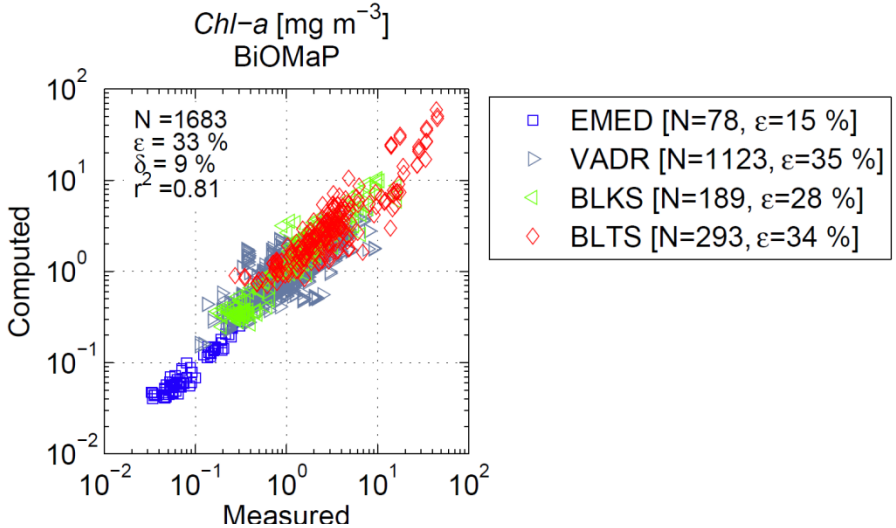

Comparisons with MERIS products

- Assessment of MERIS Chl-a estimates in the Northern Adriatic Sea, Baltic Sea and Western Black Sea on the basis of MERIS level 2 data products (3rd reprocessing)
- Compared with reference Chl-a concentration derived from MLP_{BMP} regional algorithms trained with in-situ measurements collected in the BiOMaP and CoASTS programs

MERIS image processing

- Methods
  - Retrieval of algal-1 and algal-2 Chl-a maps from MERIS L2 products
  - Application of MLP_{BMP} regional algorithms to R_{RS} images taken from the same MERIS L2 products
- Software tools
  - BEAM/Java code for data retrieval and MLP application
  - BEAM graph-processing tool (gpt) for reprojection
  - MATLAB code for data analysis and visualization

Assessment

- The scattering and the bias of MERIS Chl-a estimates $\hat{t}_i$ with respect to the corresponding MLP_{BMP} results t_i are assessed by absolute and signed percent differences ε and δ, respectively:

$$\varepsilon = 100 \frac{1}{N} \sum_{i=1}^{N} \frac{\left| \hat{t}_i - t_i \right|}{t_i} \qquad \delta = 100 \frac{1}{N} \sum_{i=1}^{N} \frac{\hat{t}_i - t_i}{t_i}$$

  where N is the total number of samples
- Only pixels in ROI(s) are considered
  - ROIs with a reduced number of noisy pixels were defined by visually inspecting product maps

Northern Adriatic Sea

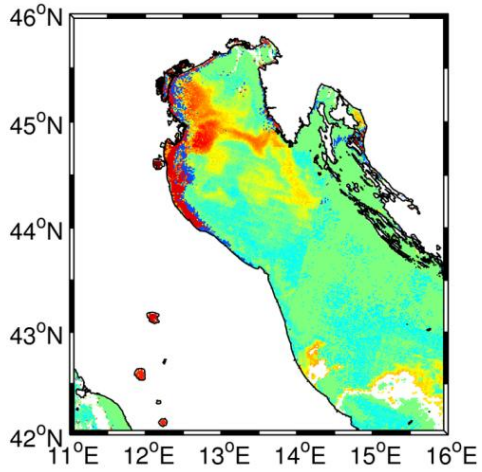

(a) BiOMaP nadr

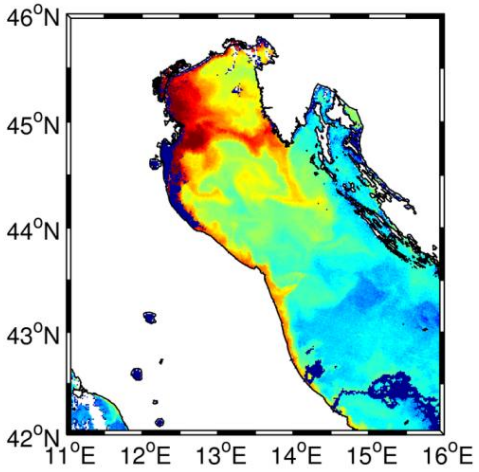

(b) MERIS algal-1

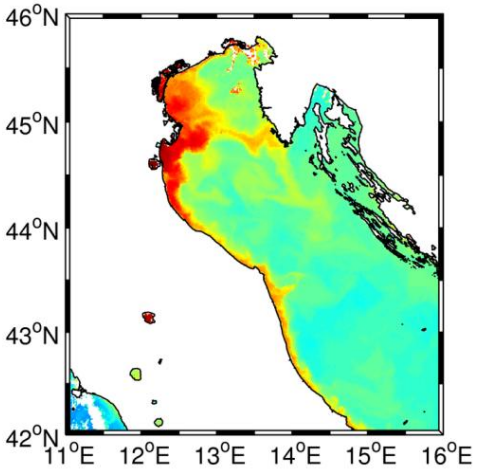

(c) MERIS algal-2

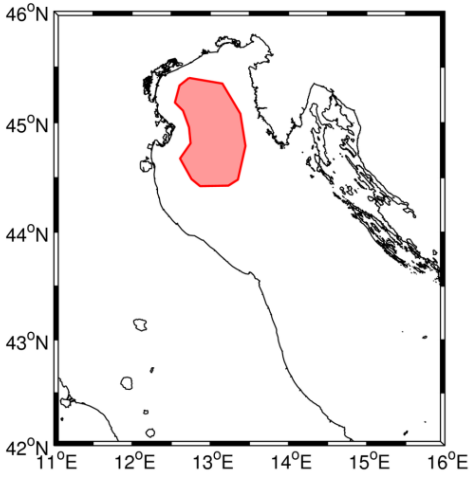

(d) ROI

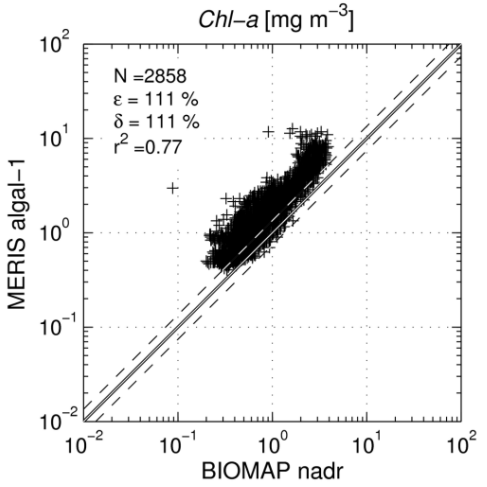

(e) BiOMaP vs. algal-1

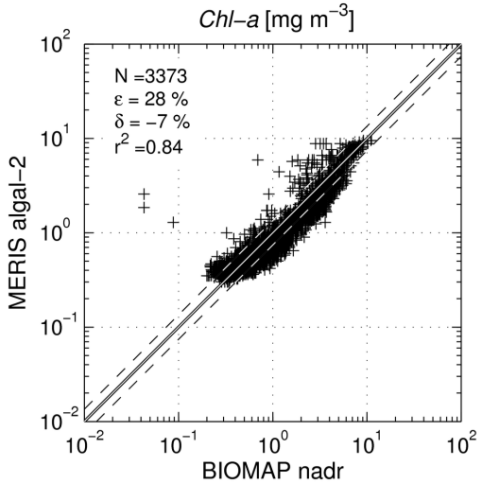

(f) BiOMaP vs. algal-2

Northern Adriatic Sea (cont.)

MERIS algal-1 vs. MLP_{BMP}

ROI	N	ε [%]	δ [%]	r^2
Total	2858	111.4	111.2	0.77

MERIS algal-2 vs. MLP_{BMP}

ROI	N	ε [%]	δ [%]	r^2
Total	3373	28.0	-7.5	0.84

Source: MER_RR__2PRACR20100824_092645_000026292092_00208_44350_0000.N1

Baltic Sea

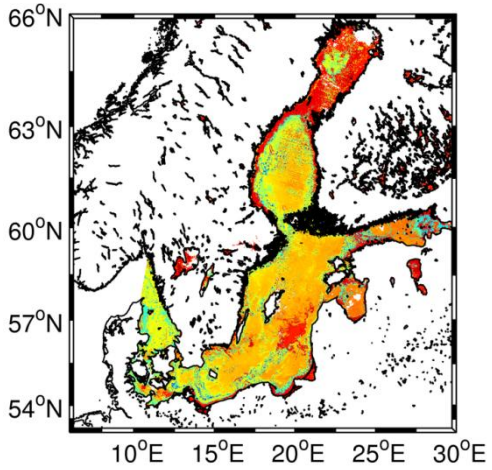

(a) BiOMaP blts

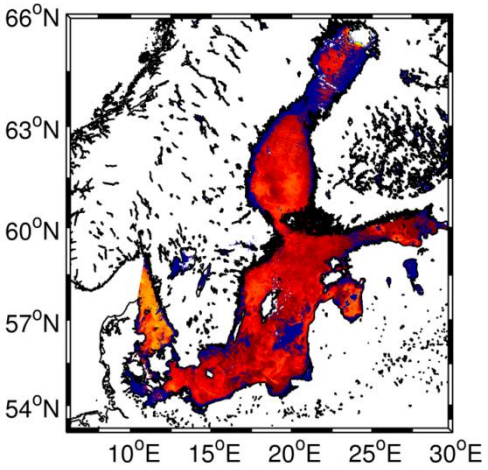

(b) MERIS algal-1

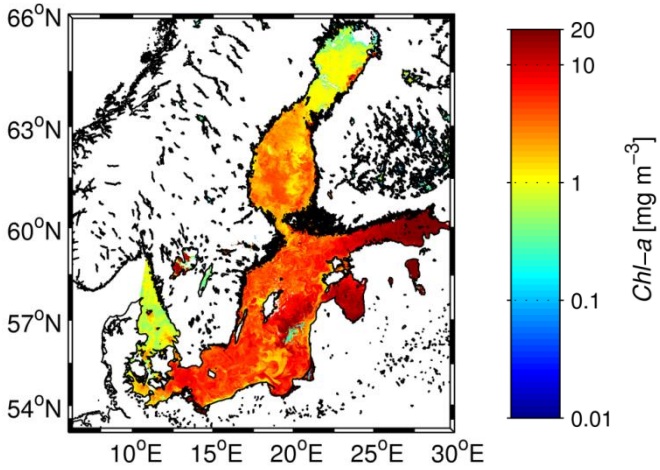

(c) MERIS algal-2

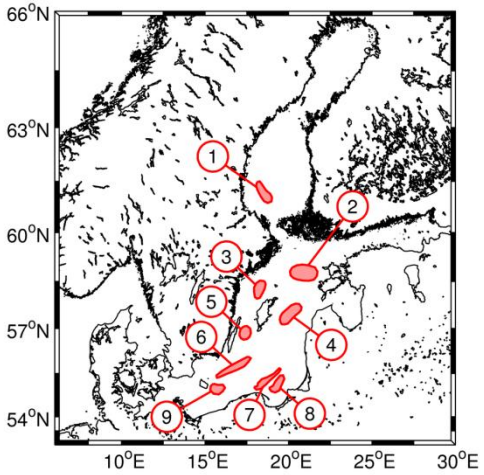

(d) ROI

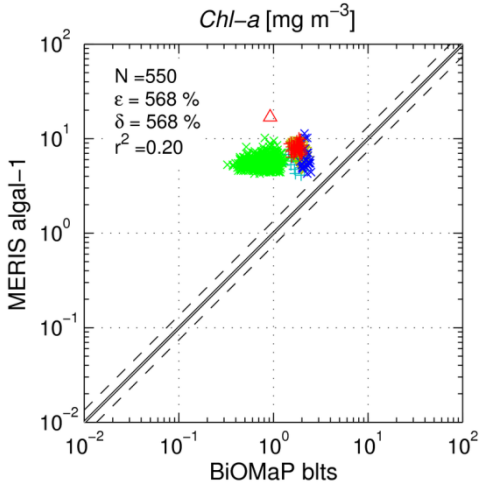

(e) BiOMaP vs. algal-1

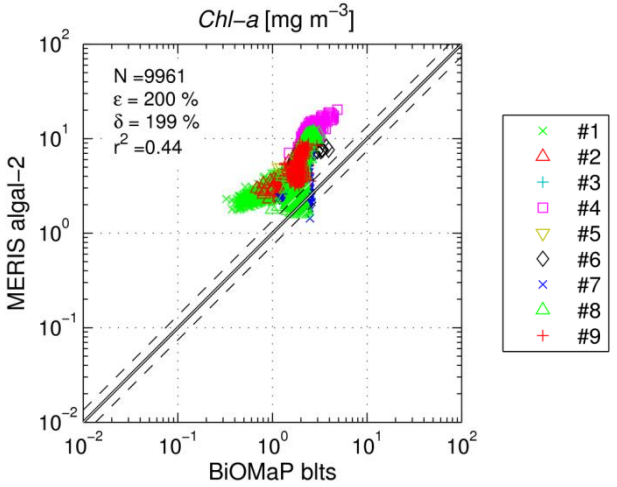

(f) BiOMaP vs. algal-2

Baltic Sea (cont.)

MERIS algal-1 vs. MLP_{BMP}

ROI	N	ε [%]	δ [%]	r^2
#1	390	679.2	679.2	0.01
#2	1	1735.9	1735.9	NaN
#3	13	238.1	238.1	0.38
#4	0	–	–	–
#5	55	279.0	279.0	0.39
#6	0	–	–	–
#7	28	175.7	175.7	0.00
#8	3	407.9	407.9	0.05
#9	60	352.4	352.4	0.02
Total	550	567.9	567.9	0.20

MERIS algal-2 vs. MLP_{BMP}

ROI	N	ε [%]	δ [%]	r^2
#1	1045	218.6	218.5	0.81
#2	2183	192.9	192.9	0.37
#3	913	166.3	166.3	0.03
#4	1511	295.4	295.4	0.62
#5	727	146.3	146.3	0.01
#6	1282	218.8	218.8	0.40
#7	826	94.7	92.4	0.22
#8	787	190.4	189.8	0.65
#9	687	183.2	183.2	0.20
Total	9961	199.6	199.4	0.44

Source: MER_RR__2PRACR20080731_092147_000026342070_00437_33557_0000.N1

Western Black Sea

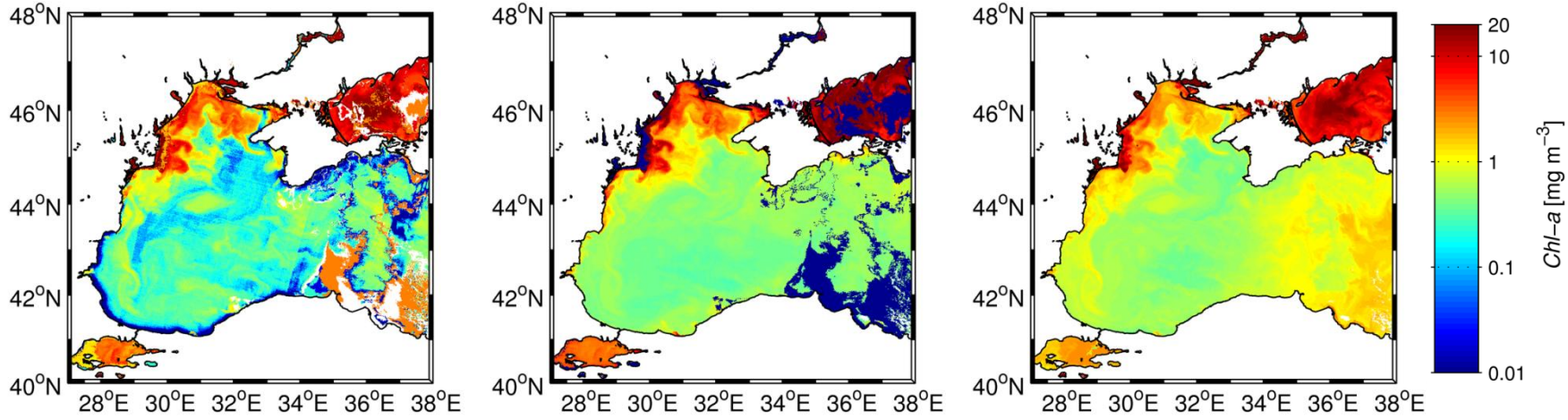

(a) BiOMaP blks (b) MERIS algal-1 (c) MERIS algal-2

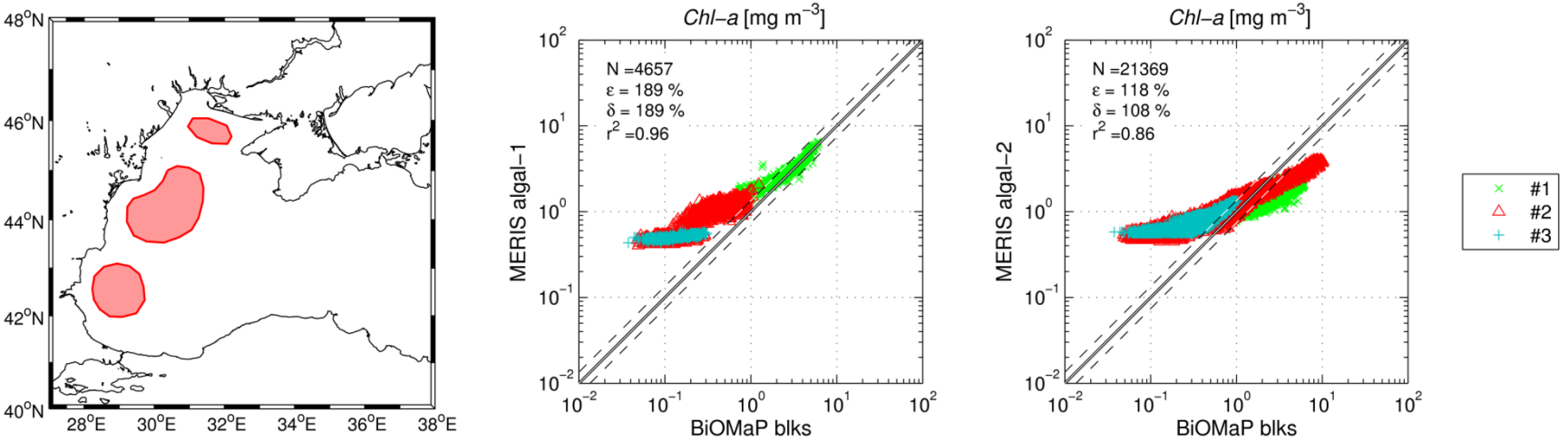

(d) ROI (e) BiOMaP vs. algal-1 (f) BiOMaP vs. algal-2

Western Black Sea (cont.)

MERIS algal-1 vs. MLP_{BMP}

ROI	N	ε [%]	δ [%]	r^2
#1	1135	51.5	49.3	0.95
#2	3033	213.6	213.6	0.83
#3	489	357.7	357.7	0.60
Total	4657	189.2	188.7	0.96

MERIS algal-2 vs. MLP_{BMP}

ROI	N	ε [%]	δ [%]	r^2
#1	2374	42.1	-27.5	0.75
#2	12295	120.7	115.5	0.87
#3	6700	141.5	141.5	0.80
Total	21369	118.5	107.8	0.86

Source: MER_RR__2PRACR20080708_081104_000021512070_00107_33227_0000.N1

Summary and conclusions

- MLPs were developed from quality assured BiOMaP and CoASTS data fulfilling the need of in-situ measurements collected in different basins with consistent instrument sets and measurement protocols
- The selected basins show a wide range of optically complex water conditions
- MERIS algal-2 Chl-a estimates exhibit a better agreement with MLP_{BMP} results than algal-1 in the considered optically complex waters

Summary and conclusions (cont.)

- Northern Adriatic Sea
  - Algal-1 overestimates MLP_{BMP} by more than 100%
  - Algal-2 and MLP_{BMP} show a substantial agreement
- Baltic Sea
  - Both algal-1 and algal-2 overestimate MLP_{BMP}
  - Algal-1 displays a clear saturation pattern
  - Specific trends at a sub-regional level
- Western Black Sea
  - A correlation between MERIS and MLP_{BMP} somehow in between to what observed in the other two basins
  - Specific trends at a sub-regional level

Foreseen studies

- Unified framework where bio-optical algorithms are developed and applied accounting for geographical distribution and optical properties to improve ocean color products retrieval
- Automated ROI selection and data processing (time series)
- Extension of the analysis to the absorption of the yellow substance (a_{ys}) and concentration of the total suspended matter (TSM)
- Extension of the analysis to additional European Seas (e.g., Atlantic off Portugal)

E.g.: Atlantic off Portugal

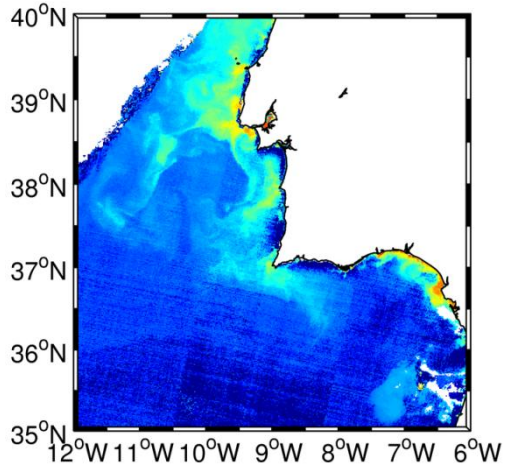

(a) BiOMaP allb

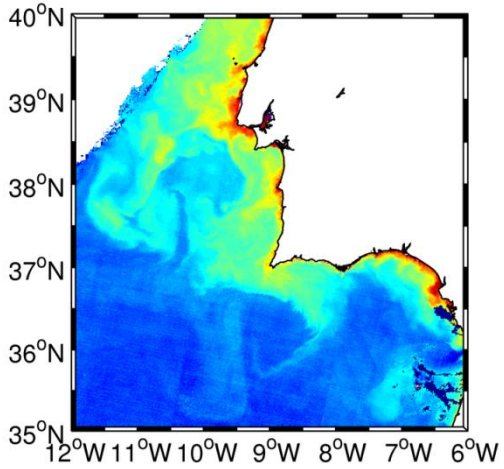

(b) MERIS algal-1

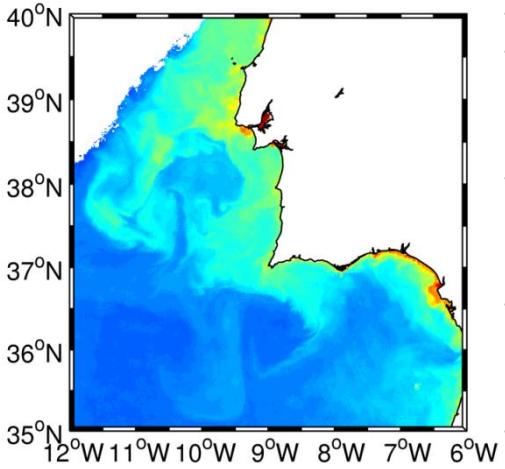

(c) MERIS algal-2

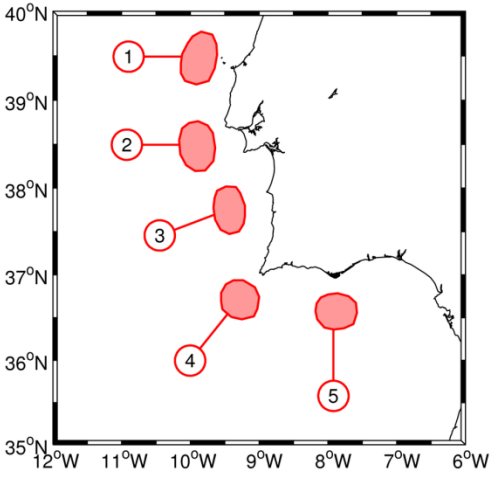

(d) ROI

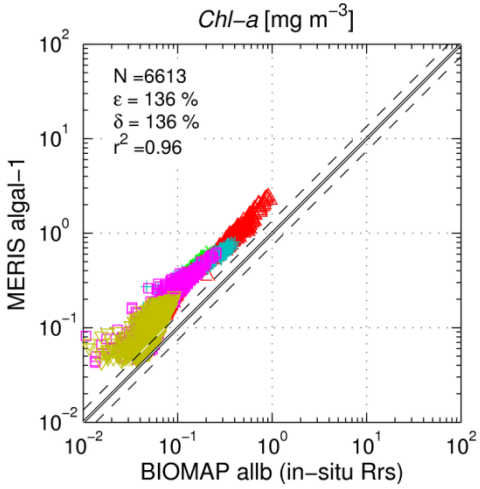

(e) BiOMaP vs. algal-1

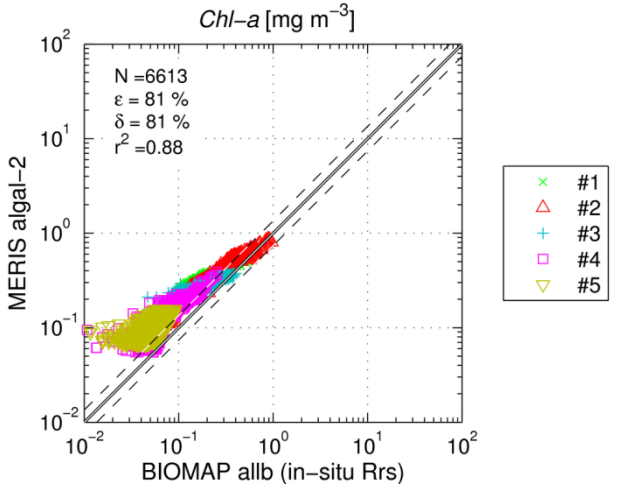

(f) BiOMaP vs. algal-2

Source: MER_RR__2PRACR20100825_103551_000026292092_00223_44365_0000.N1

E.g.: Atlantic off Portugal (cont.)

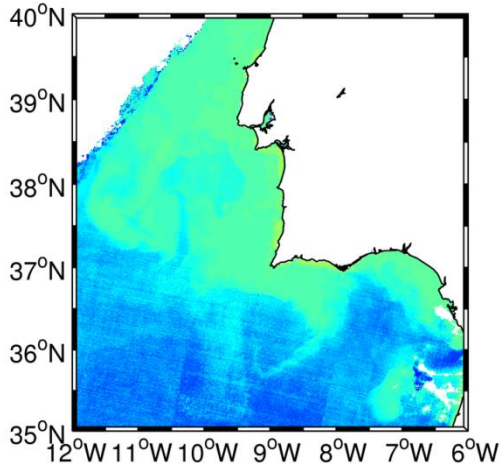

(a) BiOMaP emed

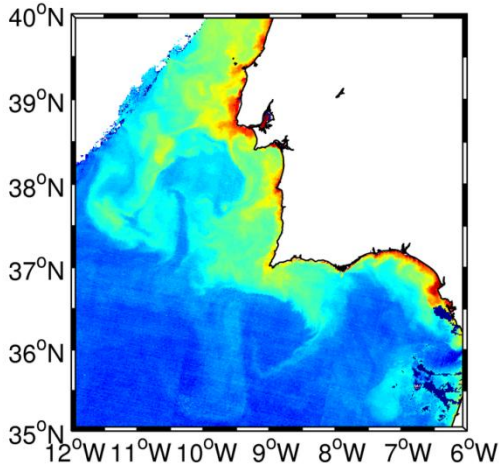

(b) MERIS algal-1

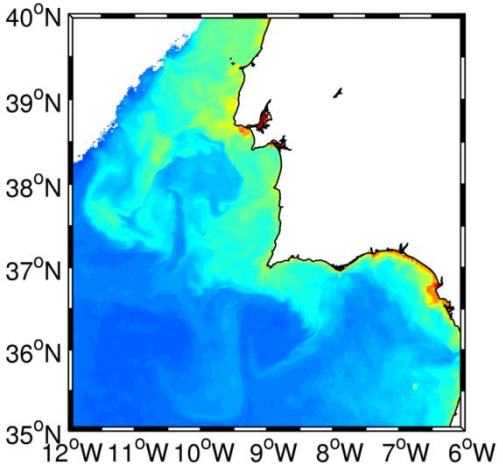

(c) MERIS algal-2

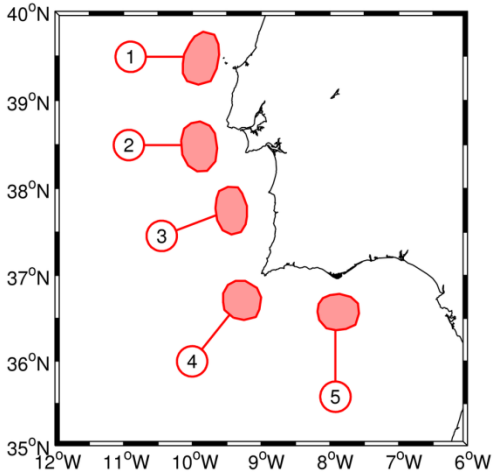

(d) ROI

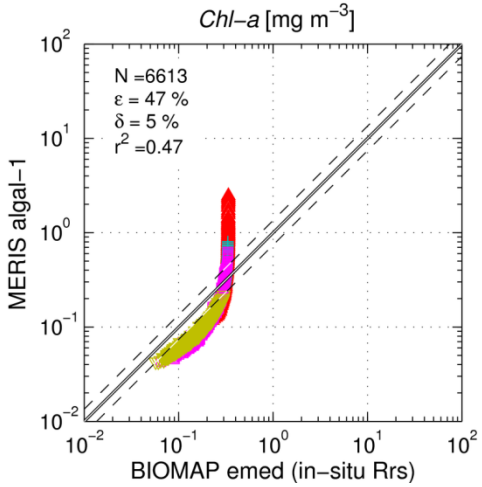

(e) BiOMaP vs. algal-1

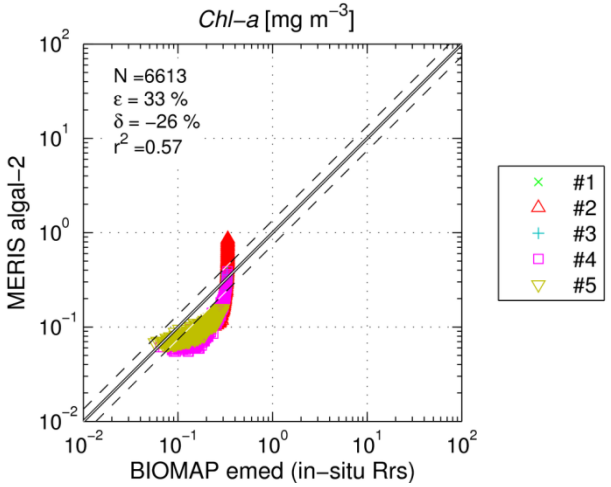

(f) BiOMaP vs. algal-2

E.g.: Atlantic off Portugal (cont.)

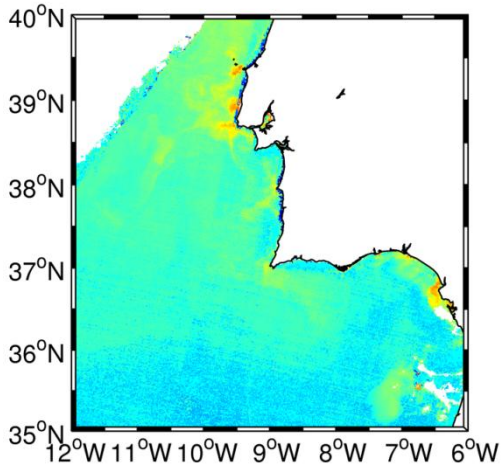

(a) BiOMaP nadr

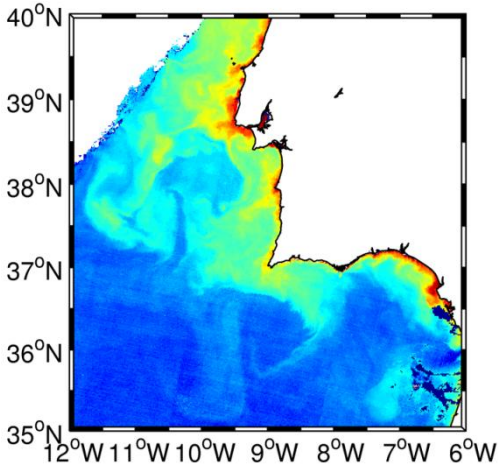

(b) MERIS algal-1

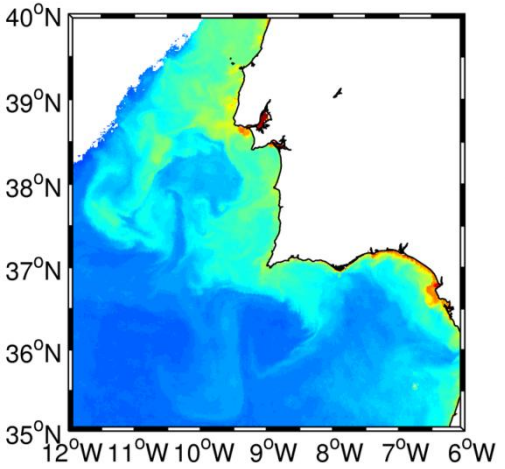

(c) MERIS algal-2

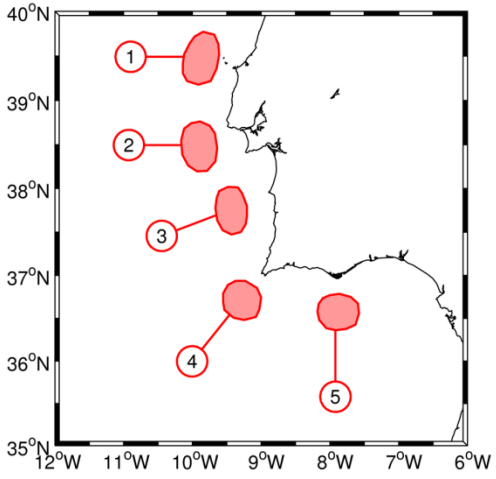

(d) ROI

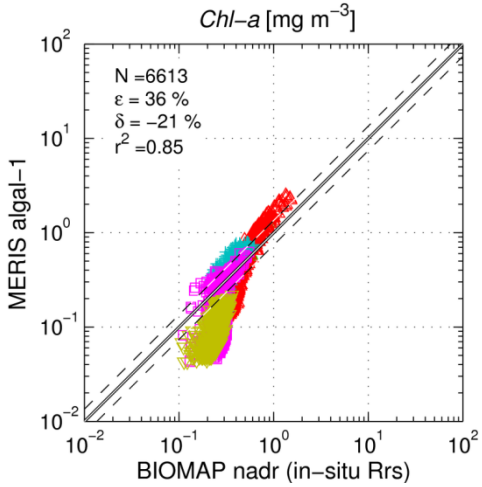

(e) BiOMaP vs. algal-1

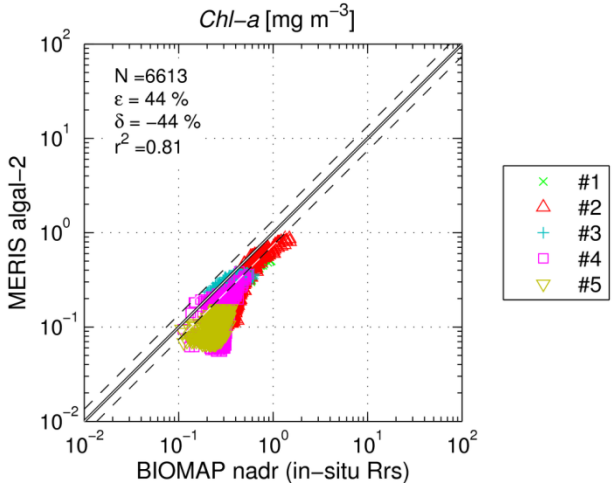

(f) BiOMaP vs. algal-2

Acknowledgments

- European Space Agency through contract number C22576.
- Geo-Info project funded by the Portuguese Foundation for Science and Technology (FCT), Ministry of Science, Technology and Higher Education

Selected publications

- D'Alimonte, D. & Zibordi, G. Statistical Assessment of Radiometric Measurements from Autonomous Systems IEEE Trans. Geosc. Rem. Sens., 2006, Vol. 44(3), pp. 719-728
- D'Alimonte, D., Zibordi, G. & Berthon, J.-F. A Statistical Index of Bio-optical Sea-water Types IEEE Trans. Geosc. Rem. Sens., 2007, Vol. 45, pp. 2644-2651
- D'Alimonte, D., Zibordi, G. & Berthon, J.-F. Determination of CDOM and NPPM Absorption Coefficient Spectra from Coastal Water Remote Sensing Reflectance IEEE Trans. Geosc. Rem. Sens., 2004, Vol. 42(8), pp. 1770-1777
- D'Alimonte, D., Zibordi, G., Kajiyama, T. & Cunha, J.C. Monte Carlo code for high spatial resolution ocean color simulations Appl. Opt., OSA, 2010, Vol. 49(26), pp. 4936-4950
- D'Alimonte, D., Zibordi, G. & Melin, F. Statistical Method for Generating Cross-Mission Consistent Normalized Water-Leaving Radiances IEEE Trans. Geosc. Rem. Sens., IEEE, 2008, Vol. 46(12), pp. 4075-4093
- Kajiyama, T., D'Alimonte, D. & Cunha, J.C. Performance prediction of ocean color Monte Carlo simulations using multi-layer perceptron neural networks International Conference on Computational Science (ICCS 2011)
- Kajiyama, T.; D'Alimonte, D.; Cunha, J. C. & Zibordi, G. High-Performance Ocean Color Monte Carlo Simulation in the Geo-info Project PPAM, 2009, 370-379
- Zibordi, G., Berthon, J.-F., Mélin, F. & D'Alimonte, D. Cross-site consistent in situ measurements for satellite ocean color applications: the BiOMaP radiometric dataset Remote Sens. Environ., 2011
- Zibordi, G., Holben, B., Mélin, F., D'Alimonte, D., Berthon, J.-F., Slutsker, I. & Giles, D. AERONET-OC: An Overview Can. J. Remote. Sens., 2011

Monte Carlo simulations

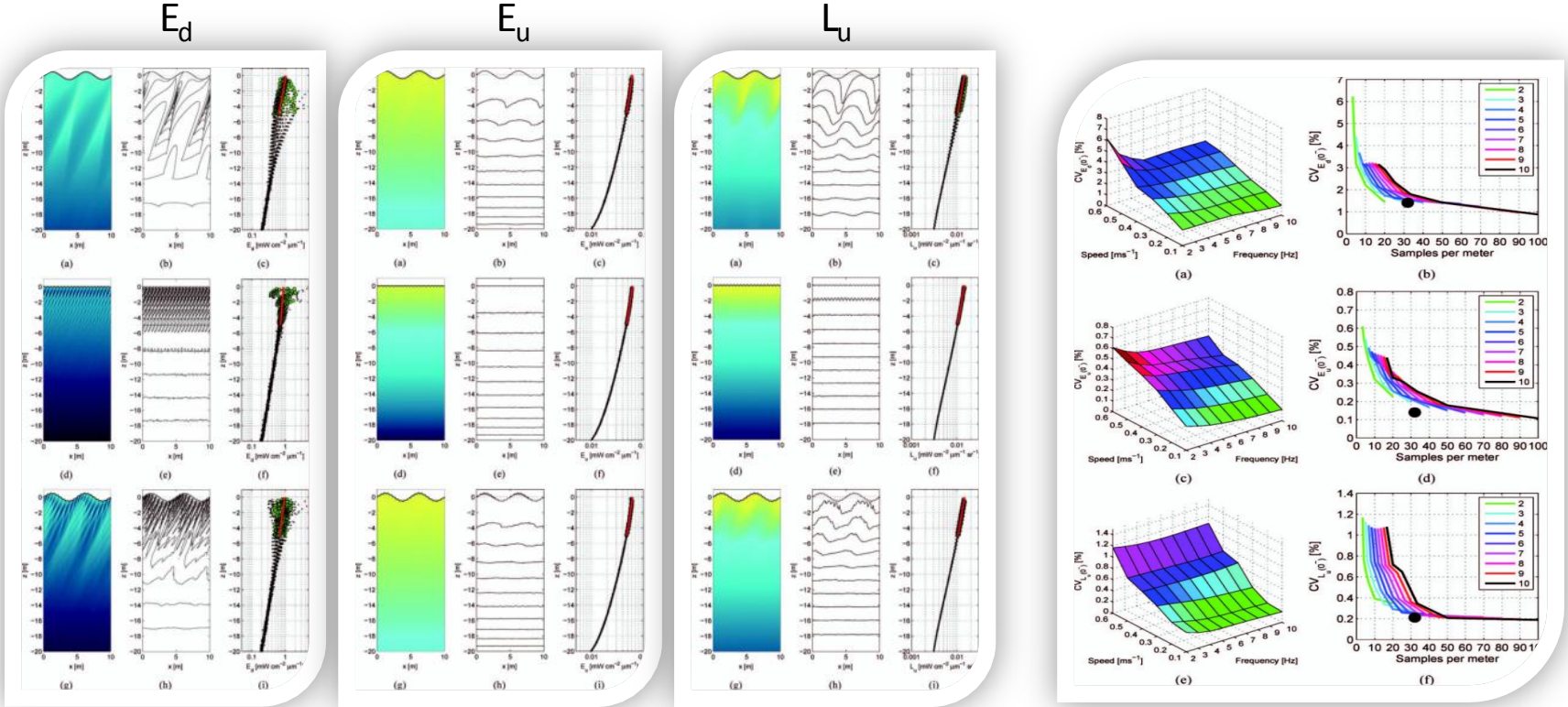

Results have shown coefficients of variation of subsurface radiometric values in the range of 0.5%–3.5% for Ed(0-), below 0.4% for Eu(0-), and up to 1.2% for Lu(0-)

Dataset selection and QA

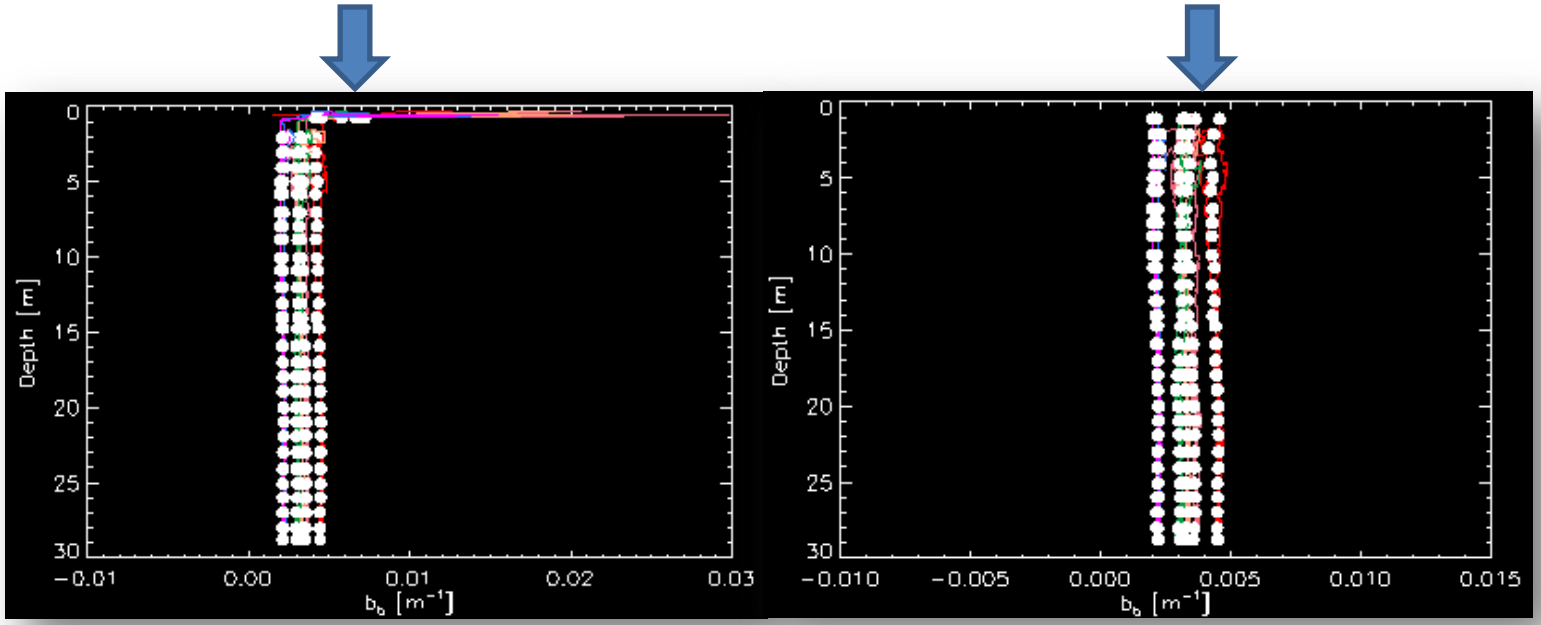

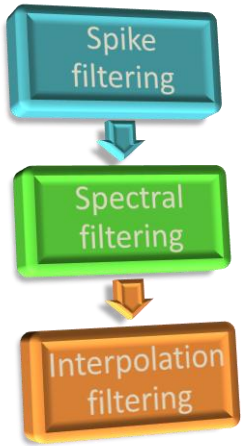

Binned data computed applying the standard moving average scheme and the optimized filtering scheme (left and right panel, respectively)